Dalton Transactions

PAPER

View Article Online
View Journal | View Issue

Halide impact on emission of mononuclear copper(I) complexes with pyrazolylpyrimidine and triphenylphosphine†

Cite this: *Dalton Trans.*, 2014, **43**, 2953

Katerina A. Vinogradova,[a] Victor F. Plyusnin,[b,c] Arkady S. Kupryakov,[b,c] Marianna I. Rakhmanova,[a] Natalia V. Pervukhina,[a] Dmitrii Yu. Naumov,[a] Lilia A. Sheludyakova,[a,b] Elena B. Nikolaenkova,[d] Viktor P. Krivopalov[d] and Mark B. Bushuev*[a,b]

Received 28th October 2013,
Accepted 28th November 2013

DOI: 10.1039/c3dt53040j

www.rsc.org/dalton

A series of mononuclear heteroleptic copper(I) halide complexes, [CuL(PPh$_3$)X] (X = Cl, Br, I), based on 4-(3,5-diphenyl-1*H*-pyrazol-1-yl)-6-(piperidin-1-yl)pyrimidine (L) and triphenylphosphine, have been synthesized by reaction between CuX (X = Cl, Br, I), L and PPh$_3$ in a molar ratio of 1/1/1 in MeCN solutions. The copper atom, showing the distorted tetrahedral environment, is bound by the *N*,*N*-chelating ligand L, triphenylphosphine and a halide ion. The complexes [CuL(PPh$_3$)Cl] and [CuL(PPh$_3$)Br] are isostructural. In CH_2Cl_2 solutions, L and the complexes [CuL(PPh$_3$)X] (X = Cl, Br, I) display a luminescence band with λ_{max} = 377 nm and a lifetime of 1.9 ns (ligand-based luminescence (LL*)). However, the complex [CuL(PPh$_3$)I] has an additional weak luminescence band with λ_{max} = 681 nm and a lifetime of 96 ns of ^{3}MLCT origin. In the solid state, L shows the splitting of the luminescence band to λ_{max} = 365 and 384 nm and a slight increase of the lifetime to 2.66 ns. Solid samples of the complexes [CuL(PPh$_3$)X] demonstrate ^{3}MLCT luminescence bands at 620 nm (X = Cl), 605 nm (X = Br) and 559 nm (X = I) with lifetimes in the range 3.6–11.2 μs, whereas the LL* band (377 nm) is absent. Quantum yields and rate constants of radiative and nonradiative processes were determined in CH_2Cl_2 solutions and in the solid state for all complexes. The luminescence quantum yield and lifetimes for the solid samples increase in the order [CuL(PPh$_3$)Cl] < [CuL(PPh$_3$)Br] < [CuL(PPh$_3$)I]. This is due to the increase of radiative decay and simultaneous suppression of nonradiative decay. The complex [CuL(PPh$_3$)I] shows a high quantum yield of 29.4% and an excited state lifetime of 11.2 μs.

Introduction

There is a growing interest in the properties of excited states of copper(I) complexes.[1] This is stimulated by a wide range of potential applications of luminescent copper(I) complexes. They are appealing objects for the development of organic light-emitting diodes,[2] oxygen sensors,[3] supramolecular assemblies, protein probes, and photovoltaic cells.[4] Copper is an abundant, inexpensive and non-toxic element which is important for potential applications. Typically, emission of copper(I) compounds results from metal-to-ligand excited states. Unfortunately, these excited states are short-lived. This leads to low quantum yields of copper(I) compounds. The examples of copper(I) complexes showing efficient emission are limited.[5,6]

Synthesis of mononuclear complexes of [Cu(*NN*)(P)Hal] and [Cu(*NN*)(PP)]$^+$ types, where *NN* denotes bidentate diimines and P and PP represent mono- and bidentate phosphines, is regarded as a tool to improve the emissive properties of copper(I) complexes based on *N*,*N*-diimine ligands.[5–7] Indeed, introducing a strong π-acidic group (like triphenylphosphine) enhances the energy gap between the highest occupied and the lowest unoccupied molecular orbitals and decreases nonradiative decay.[6] When monodentate N-ligands (N) and halido-

[a]*Nikolaev Institute of Inorganic Chemistry, Siberian Branch of Russian Academy of Sciences, 3, Akad. Lavrentiev Ave., Novosibirsk, 630090, Russia. E-mail: bushuev@niic.nsc.ru; Fax: +7 (383) 330-94-89*
[b]*Department of Natural Sciences, Novosibirsk State University (National Research University), 2, Pirogova str., Novosibirsk, 630090, Russia*
[c]*Institute of Chemical Kinetics and Combustion, Siberian Branch of Russian Academy of Sciences, 3, Institutskaya str., Novosibirsk, 630090, Russia*
[d]*N. N. Vorozhtsov Novosibirsk Institute of Organic Chemistry, Siberian Branch of Russian Academy of Sciences, 9, Akad. Lavrentiev Ave., Novosibirsk, 630090, Russia*

† Electronic supplementary information (ESI) available: Crystal data and selected bond lengths (Tables S1 and S2), X-ray powder diffraction patterns (Fig. S1), molecular structures of **2** and **3** (Fig. S2 and S3), packing diagrams of the complexes (Fig. S4–S6), IR-spectra (Fig. S7–S11). CCDC 915216–915218. For ESI and crystallographic data in CIF or other electronic format see DOI: 10.1039/c3dt53040j

ligands are used, dinuclear halido-bridged complexes $[Cu_2(\mu\text{-Hal})_2(P)_2(N)_2]$ are formed.[8]

Being a diazine system, pyrimidine shows a highly π-deficient aromatic character[9] and pyrimidine-based N-ligands are suitable candidates for synthesizing luminescent copper(I) complexes. Pyrimidine derivatives have attracted considerable attention as building blocks for the synthesis of organic π-conjugated functional materials.[9] Pyrimidine is one of the most important natural heterocycles. It is less toxic than many heterocyclic systems of synthetic origin. This is crucial for potential applications. Pyrimidine derivatives show various medicinal effects and are used in the design of pharmaceuticals.[10] In the field of pyrimidine chemistry, our research is focused on the synthesis of hybrid azolylpyrimidine-based metal complexes including complexes with (1*H*-pyrazol-1-yl)-pyrimidines.[11] The biological and pharmacological activity of pyrazolylpyrimidines and their complexes is documented.[12] Pyrazolylpyrimidines have been used as co-ligands to tune the redox properties of ruthenium(II)–bipy complexes.[13] Copper(II) complexes with these ligands reveal magnetic activity.[14] Some of these complexes have been recognized as appealing objects for the design of transition metal complexes of various nuclearities and supramolecular self-assemblies.[15,16] Although complexes with pyrazolylpyrimidines show various functional properties, there are little data available on their luminescence.[11,17]

It has previously been demonstrated that emission properties of mononuclear copper(I) complexes can be tuned by halido-ligands.[18] To the best of our knowledge, however, there are little data available on detailed comparative photophysical studies for these compounds. In this context, we endeavored to synthesize a series of heteroleptic mononuclear copper(I) halide complexes with an *N*,*N*-chelating pyrazolylpyrimidine ligand and triphenylphosphine and to study their luminescence. Here we report synthesis and comparative structural and photophysical studies of three copper(I) complexes, [CuL(PPh$_3$)X] (L = 4-(3,5-diphenyl-1*H*-pyrazol-1-yl)-6-(piperidin-1-yl)-pyrimidine; X = Cl (**1**), Br (**2**), I (**3**)), as well as the halide impact on their luminescent properties.

Experimental section

General

4-(3,5-Diphenyl-1*H*-pyrazol-1-yl)-6-(piperidin-1-yl)pyrimidine (L) was prepared according to the reported procedure.[16] All other reagents and solvents were commercially available and were used without additional purification. The syntheses of the complexes were performed under an inert atmosphere of argon. IR absorption spectra were recorded on a Scimitar FTS 2000 spectrometer (375–4000 cm^{-1}) and on a VERTEX-80 spectrometer (100–600 cm^{-1}). Elemental analysis (C, H, N) was performed with a EuroEA3000 analyzer using the standard technique. X-ray powder diffraction data were obtained with a DRON-3M automated diffractometer (R = 192 mm, Cu-K_α-radiation, Ni-filter, scintillation point detector with amplitude discrimination) at room temperature. X-ray powder diffraction patterns are given in Fig. S1, ESI.† The estimations of photoluminescence quantum yields (PLQY) for L and [CuL(PPh$_3$)X] were carried out by comparison with the spectrum of anthracene in CH_2Cl_2 solution and in the solid state (anthracene PLQY is 0.93[19]). The excitation and photoluminescence (PL) spectra of the compounds in CH_2Cl_2 solutions and in the solid state were detected using an FLS920 spectrofluorimeter (Edinburg Instruments) at room temperature. The solid samples for recording PL spectra and PL kinetics were prepared by grinding the compounds to powder between two quartz glasses. The thin layer of powder between glasses was placed at 45° to the excitation light beam. For registration of PL in the solutions, the standard 1 cm cuvette and the spectral pure CH_2Cl_2 were used. The xenon Xe900 lamp was employed as a light source to excite the steady-state PL spectra. To record PL kinetics, the laser diode EPLED-320 (λ_{ex} = 320 nm, pulse duration 600 ps) and the diode laser EPL-375 (λ_{ex} = 375 nm, pulse duration 60 ps) were applied. The PL kinetics were fitted by biexponential approximations using the FLS920 program or FAST program (Edinburgh Instruments). The optical absorption spectra were recorded on a HP 8453 spectrophotometer (Agilent Technologies).

Synthesis of [CuL(PPh$_3$)Cl] (1)

A colorless solution of CuCl (0.10 mmol, 9.9 mg) in MeCN (2 ml) was added to a hot stirred solution of L (0.10 mmol, 38.1 mg) in MeCN (2 ml). The color of the reaction mixture turned yellow-orange and a yellow precipitate appeared in *ca.* 1–2 minutes. PPh_3 (0.10 mmol, 26.2 mg) was added to the resulting mixture. The precipitate disappeared and the color of the solution turned light yellow green. After stirring the solution for 10 min, a light yellow precipitate began to form. The reaction mixture was concentrated to *ca.* 1 ml, the precipitate was filtered off, washed with MeCN and dried in the ambient air. Yield: 60.9 mg (75.0%). Anal. calc. for $C_{42}H_{38}N_5ClCuP$: C, 67.9; H, 5.1; N, 9.4. Found: C, 67.6; H, 5.1; N, 9.5%. Single crystals were obtained by slow crystallization from the mother liquor the next day.

Synthesis of [CuL(PPh$_3$)Br] (2)

Copper powder was added to a stirred solution of $CuBr_2$ (0.050 mmol, 11.2 mg) in MeCN (2 ml). When the green color of the solution disappeared, the copper powder was filtered off. The resulting colorless solution of CuBr (0.10 mmol) was added to a hot solution of L (0.10 mmol, 38.1 mg) in MeCN (3 ml). When the color of the solution became orange, a light yellow precipitate appeared. PPh_3 (0.10 mmol, 26.2 mg) was added to the reaction mixture. The precipitate disappeared and the color of the solution turned light yellow green. A light green-yellow precipitate was formed in *ca.* 10 min. The reaction mixture was concentrated to 1 ml, the precipitate was filtered off, washed with MeCN and dried in ambient air. Yield: 67 mg (85.2%). Anal. Calc. for $C_{42}H_{38}N_5BrCuP$: C, 64.0; H, 4.9; N, 8.9. Found: C, 63.7; H, 5.3; N, 8.9%. Single crystals were obtained by slow crystallization from mother liquor in 2 days.

Synthesis of [CuL(PPh$_3$)I] (3)

A solution of CuI (0.10 mmol, 19 mg) in MeCN (1 ml) was added to a hot stirred solution of L (0.10 mmol, 38 mg) in MeCN (2 ml). The color of the resulting solution became bright yellow and a yellow precipitate formed. PPh_3 (0.10 mmol, 26.2 mg) was added to the reaction mixture. The precipitate disappeared and the color of the solution turned light yellow green. A light green-yellow precipitate was formed in *ca.* 2–3 min. The reaction mixture was concentrated to 1 ml, the precipitate was filtered off, washed with MeCN and dried in ambient air. Yield: 76 mg (91%). Anal. Calc. for $CuC_{42}H_{38}N_5PI$: C, 60.5; H, 4.6; N, 8.4. Found: C, 60.3; H, 5.2; N, 8.3. Single crystals were obtained by slow crystallization from MeCN solution containing [CuL(PPh$_3$)I] and PPh_3 in a 1 : 1 molar ratio.

X-ray structure analysis

Intensity data were collected on a Bruker Nonius X8Apex CCD diffractometer equipped with a graphite monochromated Mo-K$_\alpha$ (λ = 0.71073 Å) radiation source. The SMART software was used for data collection and also for indexing the reflections and determining the unit cell parameters; the collected data were integrated using the SAINT[20] software and SADABS[20] for absorption correction. The structures were solved by direct methods and refined by full-matrix least-squares calculations using the SHELXTL software.[20] All the non-H atoms were refined in the anisotropic approximation. Hydrogen atoms were placed in idealized positions and refined using a riding model to the atom to which they are attached. Crystallographic data and refinement details are displayed in Table S1, ESI.† The bond lengths and angles are given in Table S2, ESI.†

Results and discussion

Synthetic aspects

The complexes were synthesized as follows. In the first stage, the copper(I) halides were reacted with L in MeCN solutions to yield poorly soluble precipitates of [CuLX] (X = Cl, Br) and [Cu$_2$L$_2$I$_2$].[11] In the second stage, the resulting mixtures were treated with one equivalent of PPh_3. This resulted in the dissolution of initially precipitated copper(I) complexes and, further, in precipitation of heteroleptic complexes [CuL(PPh$_3$)X] (Scheme 1). The solid samples of complexes were stable in ambient air. Although the complexes were synthesized under an inert atmosphere, their solutions in MeCN, MeCN–CHCl$_3$ and CH_2Cl_2 were stable in air for a long time. No sign of oxidation was detected for the solutions upon several days of storage. The single crystals of **1** and **2** were grown from MeCN solutions of the corresponding complexes. Surprisingly, crystallization of **3** in similar conditions afforded only crystals of the dinuclear complex [Cu$_2$L$_2$I$_2$].[11] To obtain single crystals of **3**, it was necessary to crystallize **3** from MeCN in the presence of an additional equivalent of PPh_3. The phase purity of the powder samples was confirmed by X-ray powder diffraction (Fig. S1, ESI†).

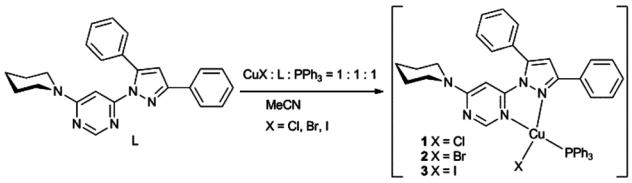

Scheme 1 Synthesis of the complexes.

Structural aspects

The complexes **1** and **2** are isostructural. They crystallize in the triclinic space group $P\bar{1}$. Instead, their iodide analog, **3**, adopts the monoclinic space group $P2_1/c$. The molecule of **3** (with the atom numbering scheme) is shown as an example in Fig. 1. The molecules of **1** and **2** are depicted in Fig. S2 and S3, ESI.† The geometry around each copper atom is distorted tetrahedral, CuN_2PX. The molecules of L are coordinated to copper atoms through N^2(pyrazole) and N^3(pyrimidine) atoms adopting thus a bidentate chelating coordination mode. As a result of the ligand coordination, the $CuCN_3$ chelate cycles are closed. The angles N(13)–Cu(1)–N(11) are the smallest in the coordination sphere which is dictated by chelating coordination of L. There is a noticeable halide impact on the geometry of the copper(I) coordination sphere. Indeed, the mean Cu–N bond distance decreases slightly in the order: **1** (2.125 Å), **2** (2.1085 Å), **3** (2.1005 Å). This correlates with the elongation of the Cu–Hal bond and may result from steric reasons. In turn, the shortening of Cu–N bond lengths leads to the increase in the corresponding N(13)–Cu(1)–N(11) angles. The Cu–P bond distances for **1** and **2** are practically identical with each other, but this bond for **3** is somewhat elongated (the elongation exceeds the experimental error).

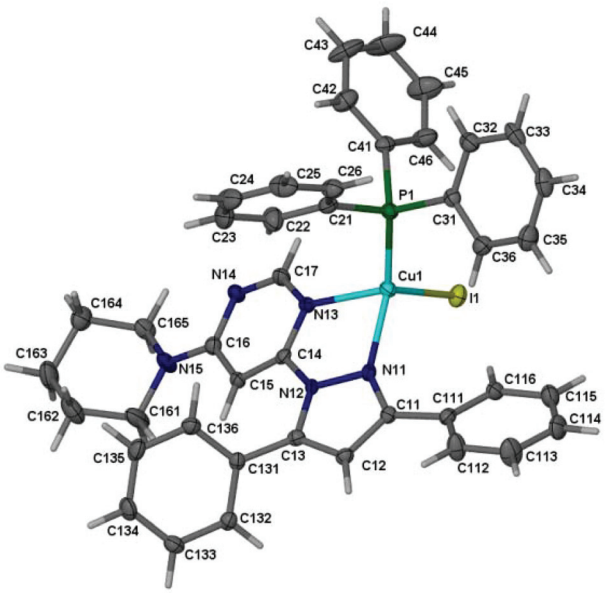

Fig. 1 Molecular structure of **3**.

Table 1 Main vibrational frequencies in IR spectra (cm^{-1})

Compound	ν(CH)	$\nu(CH_2)$	$(\nu + \delta)_{ring}$	CPC	ν(Cu–N)	ν(Cu–X)
1	3062, 3045, 3032, 3003	2930, 2860, 2848	1604, 1591, 1555, 1536, 1504, 1487	521, 509, 493	282, 261 (mixed with Cu–Cl)	261 (mixed with Cu–N)
2	3059, 3043, 3030, 3002	2928, 2860, 2849	1602, 1573, 1554, 1536, 1503, 1462	521, 509, 491	281, 257	204
3	3060, 3041, 3029, 3015, 2999, 2987	2924, 2853	1598, 1566, 1537, 1500, 1481	522, 505, 492	271, 255	150
L	3059, 3009	2930, 2827	1591, 1552, 1531, 1487	—	—	—
PPh_3			1582, 1480	545, 515, 500	—	—

Importantly, the pseudo-tetrahedral geometry of the coordination core becomes less angularly distorted on going from the chlorido- to iodido-complex. This is reflected by the sum of valence angles in the coordination sphere of the copper atom: 643.22° for **1**, 643.55° for **2** and 646.96° for **3**. For a perfect tetrahedron this sum is 657°. There is another way to measure the degree of deviation of a metal atom from an ideal tetrahedral geometry. For the ideal tetrahedron CuABCD the sum of dihedral angles between the planes A–Cu–B and C–Cu–D, A–Cu–C and B–Cu–D, B–Cu–C and A–Cu–D is 270°. This sum is 230.08° for **1**, 232.35° for **2** and 237.09° for **3**.

Packing diagrams of **1–3** are depicted in Fig. S4–S6, ESI.† The coordinated halide atom in the crystal structures of **1–3** acts as a hydrogen bond acceptor and forms a hydrogen bond with the CH-groups of the adjacent complex molecules (for **1**: Cl(1)···H′(34) 2.893 Å, Cl(1)···C(34)′ 3.561 Å; Cl(1)···H(44)′ 2.874 Å, Cl(1)···C(44)′ 3.640 Å; Cl(1)···H(16A)′ 2.850 Å, Cl(1)···C(165)′ 3.777 Å; for **2**: Br(1)···H(44A)′ 2.760 Å, Br(1)···C(44A)′ 3.562 Å; Br(1)···H(24)′ 2.971 Å, Br(1)···C(24)′ 3.637 Å; Br(1)···H(16D)′ 2.993 Å, Br(1)···C(165)′ 3.893 Å; for **3**: I(1)···H(113)′ 3.161 Å, I(1)···C(113)′ 3.927 Å; I(1)···H(134)′ 3.081 Å, I(1)···C(134)′ 3.883 Å). The structures of **1** and **2** demonstrate short contacts between the N(14) atom of the pyrimidine ring and the N(15) atom of the piperidino-ring (3.350 Å for **1**; 3.423 Å for **2**). Finally, in the crystal structure of **3**, the molecules are arranged in the (100) plane according to parquet packing (Fig. S6, ESI†).

IR-spectra

The IR spectra of these compounds are similar (Table 1, Fig. S7–S11, ESI†). The positions of stretching-deformation vibrations of the heteroaromatic rings, $(\nu + \delta)_{ring}$, in the IR spectra of these complexes are changed in comparison with the spectrum of L. The far-IR spectra of the complexes exhibit the bands of Cu–N and Cu–X (X = Cl, Br, I) stretching vibrations. These observations are consistent with the coordination of the L molecules and halide ions. The bands of the C–P–C vibrations of coordinated PPh_3 molecules are observed in the region 530–450 cm^{-1}.

Intriguingly, the bands of ν(Cu–N) vibrations slightly shift to low frequencies on going from **1** to **3**. This is indicative of some weakening of the Cu–N bonds. The trend is opposite to that expected on the base of structural data for the complexes showing the shortening of the Cu–N bond lengths in the same order. This low frequency shift correlates with the increase in the π-accepting ability of halide ions and may reflect the possible weakening of Cu–L back-bonding.

Importantly, this trend is in line with the slight overall decrease of the vibrational frequencies in the order **1** > **2** > **3** including decrease of frequencies of high-frequency oscillators (CH- and CH_2-groups) and heteroaromatic rings (Table 1 and Fig. S7–S11, ESI†).

UV-Vis spectra, PL spectra and kinetics of luminescence

The bands in the absorption spectra of the $[Cu(NN)(PPh_3)_2]^+$ and $[Cu(NN)(PPh_3)X]$ systems (where *NN* stands for *N*,*N*-chelating ligands) can be assigned to metal-to-ligand charge transfer (MLCT) transitions because the color and the bands do not occur in the spectra of the complexes $[Cu(PPh_3)_2]^+$ and free *N*,*N*-ligands. Moreover, analogous MLCT transitions are well-known for $[Cu(NN)_2]^+$ complexes.[21]

Fig. 2 shows the optical absorption spectra of L and $[CuL(PPh_3)X]$ in CH_2Cl_2 solutions. The positions of absorption bands maxima are listed in Table 2. It should be noted that the absorption of the complexes $[CuL(PPh_3)X]$ in the spectral interval 230–350 nm can represent overlapping of charge transfer (metal-to-ligand (MLCT) or ligand-to-metal (LMCT)) and intraligand (LL*) bands as the free L has a wide band with a maximum at 257 nm and shoulders at 293 and 320 nm.

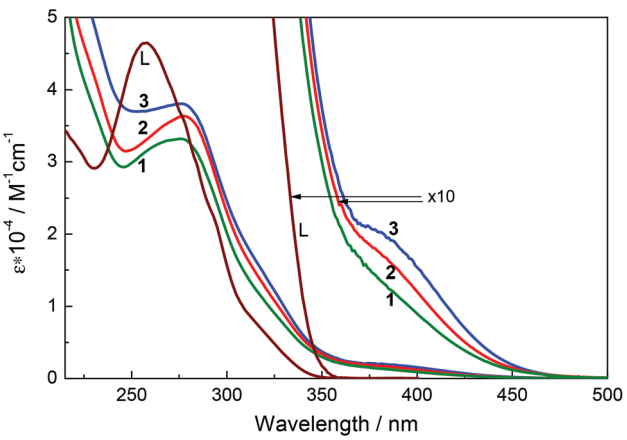

Fig. 2 Optical absorption spectra of L, $[CuL(PPh_3)Cl]$ (**1**), $[CuL(PPh_3)Br]$ (**2**) and $[CuL(PPh_3)I]$ (**3**) in CH_2Cl_2.

Table 2 The maxima of absorption bands of L and [CuL(PPh$_3$)X] compounds in CH_2Cl_2

Compound	The maxima of absorption bands/nm (absorption coefficient/M^{-1} cm^{-1})		
L	257 (46 500)	293sh (22 500)	320sh (7200)
[CuL(PPh$_3$)Cl]	276 (33 150)	318sh (10 720)	375sh (1530)
[CuL(PPh$_3$)Br]	278 (36 370)	318sh (13 530)	375sh (1860)
[CuL(PPh$_3$)I]	277 (38 020)	316sh (15 990)	375sh (2100)

However, a band (as a shoulder) for the complexes [CuL(PPh$_3$)X] at 375–380 nm is determined only by the MLCT transition. So, excitation of the complexes [CuL(PPh$_3$)X] at 375–450 nm will lead to emission from the MLCT (Cu → L) excited state.

Excitation of free L in CH_2Cl_2 results in the luminescence band with a maximum at 377 nm and an excited state lifetime of 1.94 ns. PLQY and rate constants of radiative and nonradiative processes are listed in Table 3. Fig. 3 demonstrates the excitation and PL spectra of [CuL(PPh$_3$)I] in CH_2Cl_2. All complexes [CuL(PPh$_3$)X] exhibit the same luminescence bands at 377 nm (LL* luminescence) with similar lifetimes and PLQYs (Table 3). However, upon excitation in the range of the pure MLCT band (375–450 nm), [CuL(PPh$_3$)I] shows a new wide and weak PL band with a maximum at 681 nm (Fig. 3) and an excited state lifetime of about 100 ns. Fig. 4 shows PL kinetics of [CuL(PPh$_3$)I] in CH_2Cl_2 in the range of LL* (377 nm) and ^{3}MLCT (681 nm) transitions. The long time of about 100 ns points to the emission from the ^{3}MLCT state with low PLQY due to the low radiative rate constant (Table 3). The complex [CuL(PPh$_3$)Br] also demonstrates the weak emission from the ^{3}MLCT state at 680 nm with a lower quantum yield (≤0.001) (Table 3).

Fig. 5 shows the excitation and PL spectra of L and [CuL(PPh$_3$)X] in the solid state (Fig. 6 displays PL kinetics for this case). The positions of luminescence bands maxima, PLQYs and lifetimes are presented in Table 4. The powder of L shows PL maxima at 365 and 385 nm and non-exponential kinetics. To fit the kinetic curves, the biexponential approximation, which is the best way and agrees with experimental curves, was used (eqn (1)).

$$I(t) = A_1 e^{-\frac{t}{\tau_1}} + A_2 e^{-\frac{t}{\tau_2}} \quad (1)$$

For the excitation of PL in time-resolved experiments, the EPL-375 diode laser was used. The convolution with the response function which was recorded with a scattering on quartz frosted glass allows determining the PL lifetimes of about 20 ps. The percent of emitted quanta in every exponent is determined by the $A_i\tau_i$ product. The lifetime (τ) and quantum yield (φ) of PL are determined by eqn (2) and (3).

$$\tau = \frac{1}{k_r + k_{nr}} \quad (2)$$

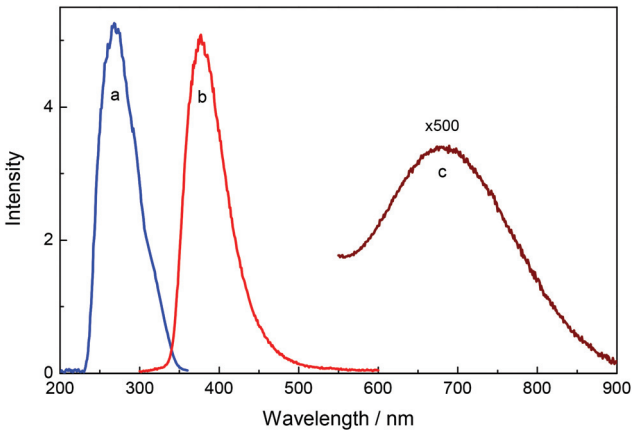

Fig. 3 Excitation (a) and PL (b, c) spectra of [CuL(PPh$_3$)I] in CH_2Cl_2. a – registration at 377 nm; b – excitation at 270 nm; c – excitation at 420 nm.

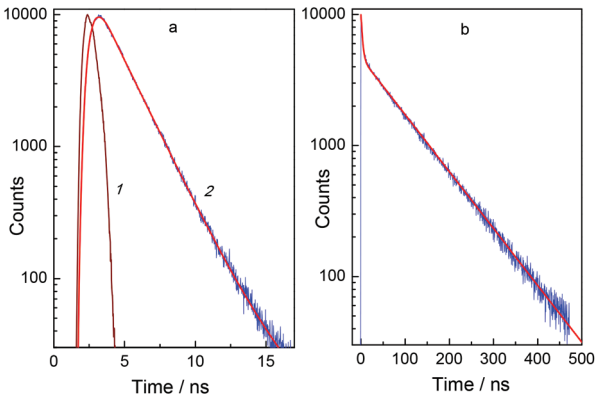

Fig. 4 Kinetic curves of PL for [CuL(PPh$_3$)I] in CH_2Cl_2. a – excitation at 280 nm and registration at 377 nm; b – excitation at 375 nm and registration at 680 nm. Solid lines are the fitting in biexponential approximations (results of fitting are presented in Table 3).

Table 3 The maxima of bands, quantum yields and lifetimes of PL for L and [CuL(PPh$_3$)X] compounds in CH_2Cl_2. The fitting of kinetic curves is in biexponential approximation. In the last two columns the rate constants of radiative and nonradiative transitions are presented

Compound	λ_{max}/nm	φ	τ_1/ns	$A_1\tau_1$%	τ_2/ns	$A_2\tau_2$%	k_r/s^{-1}	k_{nr}/s^{-1}
L	377	0.34	1.94	99	3.8	1	1.75×10^8	3.40×10^8
[CuL(PPh$_3$)Cl]	377	0.31	1.92	98	4.3	2	1.60×10^8	3.60×10^8
[CuL(PPh$_3$)Br]	377	0.30	1.86	97	4.1	3	1.61×10^8	3.75×10^8
	~691	~0.001	25.6	100	—	—	$\sim 1 \times 10^4$	$\sim 1 \times 10^7$
[CuL(PPh$_3$)I]	377	0.295	1.94	98	6.7	2	1.52×10^8	3.63×10^8
	681	~0.003	96	100	—	—	$\sim 3 \times 10^4$	$\sim 1 \times 10^7$

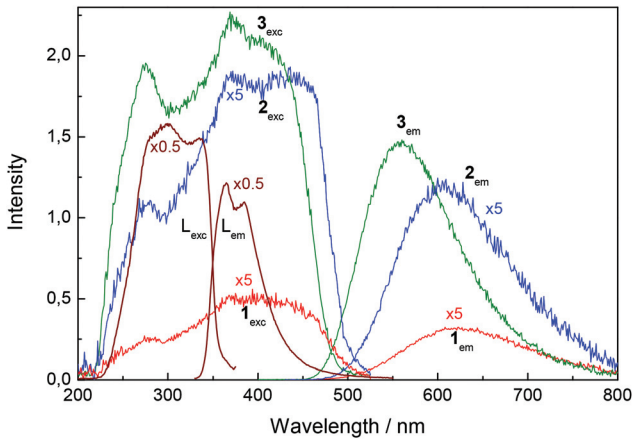

Fig. 5 Excitation (L_{exc}, 1_{exc}, 2_{exc}, 3_{exc}) and PL spectra (L_{em}, 1_{em}, 2_{em}, 3_{em}) of powdered samples of *L*, [CuL(PPh$_3$)Cl] (**1**), [CuL(PPh$_3$)Br] (**2**) and [CuL(PPh$_3$)I] (**3**).

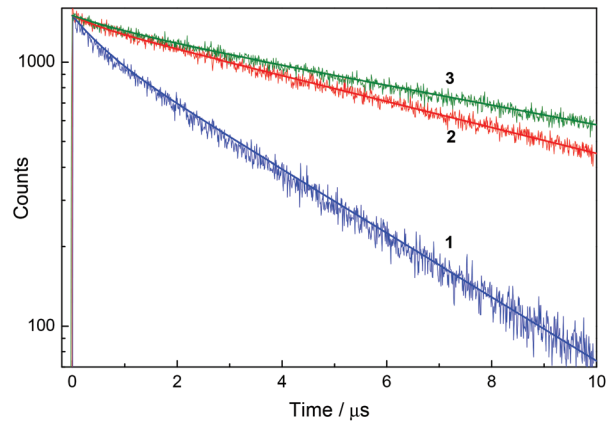

Fig. 6 Kinetic curves of PL for the complexes [CuL(PPh$_3$)Cl] (**1**), [CuL(PPh$_3$)Br] (**2**) and [CuL(PPh$_3$)I] (**3**) in solid state. Excitation at 375 nm and registration at 620 (**1**), 605 (**2**) and 560 (**3**) nm. Solid lines are the fitting in biexponential approximations (results of fitting are presented in Table 4).

$$\varphi = \frac{k_r}{k_r + k_{nr}} = k_r\tau \qquad (3)$$

where k_r and k_{nr} are the rate constants of radiative and nonradiative transitions, respectively, from the excited state to the ground state.

For the powder of L, the time of main exponent (τ_2 = 2.66 ns, 94.2% of emitted quanta) is close to the PL lifetime for L in CH_2Cl_2 (τ = 1.94 ns). PLQYs in both cases are also close to each other (Tables 3 and 4). The shorter component with a lifetime of 0.73 ns (only 5.8% of emitted quanta) for the free L ligand powder can be due to the presence of surface molecules for microcrystals. Therefore, the photophysical parameters of a free L do not change much on going from the solution to the solid state.

For [CuL(PPh$_3$)X], the PL band at 377 nm, which was observed in the CH_2Cl_2 solution spectra, disappears in the solid state. Instead, new luminescence bands in the 560–620 nm range (Table 4) are observed. They are analogous to the weak PL bands at 680 nm for [CuL(PPh$_3$)I] and [CuL(PPh$_3$)Br] in CH_2Cl_2. So, these PL bands can be assigned to the transitions from the ^{3}MLCT state to the ground state. The long PL lifetimes of about 3.6–11.2 μs also point to this attribution (Table 4). The biexponential approximations were used to fit the PL kinetic curves for [CuL(PPh$_3$)X] in the solid state, as was done in the case of the powder of L. The time of the first exponent is τ_1 = 0.6–1.2 μs; however its amplitude is small (<4% of emitted quanta, Table 4). The time of the second exponent is τ_2 = 3.6–11.6 μs (>96% of total intensity). These times were used to calculate the rate constants of radiative and nonradiative transitions (Table 4).

Short PL times (τ_1 = 0.6–1.2 μs) of the first exponent can be explained by the existence of complex molecules on the surface of microcrystals with the faster nonradiative transitions. Recently, Coppens with colleagues published two articles devoted to photophysics of [Cu(phen)(PPh$_3$)$_2$][BF$_4$] in the solid state.[22] The biexponential PL decay of [Cu(phen)(PPh$_3$)$_2$]$^+$ complex was explained by the authors by the existence of two different geometries of the complex in the excited ^{3}MLCT state (due to different local molecular environments).

The PLQY of ^{3}MLCT luminescence of **3** in the solid state is comparable to the quantum yield of LL* luminescence of this complex in CH_2Cl_2. However, the microsecond lifetime of ^{3}MLCT luminescence shows the decrease of the rate constants of radiative and nonradiative transitions by four and three orders, respectively (Table 4). It is interesting that, the $k_r \sim 10^4$ s^{-1} values for ^{3}MLCT luminescence of **3** are close to each other both in CH_2Cl_2 solution (681 nm) and in the solid state (559 nm). Importantly, there is a noticeable suppression of nonradiative decay for ^{3}MLCT luminescence on going from the solution to the solid state for **2** and **3**. This is accompanied by an increase in the excited state lifetime and PLQY. The Stokes shift reflecting the degree of inner sphere reorganization[23] decreases in the same order. The reason for the suppression of

Table 4 The maxima of bands, quantum yields and lifetimes of PL for L and [CuL(PPh3)X] as powder samples with an excitation at 320 nm. The fitting of kinetic curves is in biexponential approximations. In last two columns the rate constants of radiative and nonradiative transitions are presented

Compound	λ_{max}/nm	φ_f	τ_1/μs	$A_1\tau_1$/%	τ_2/μs	$A_2\tau_2$/%	k_r/s^{-1}	k_{nr}/s^{-1}
L	365, 384	0.233	0.73×10^{-3}	5.8%	2.66×10^{-3}	94.2%	0.88×10^8	2.88×10^8
[CuL(PPh$_3$)Cl]	620	0.0169	0.60 ± 0.04	4%	3.59 ± 0.03	96%	0.47×10^4	2.74×10^5
[CuL(PPh$_3$)Br]	605	0.0627	0.58 ± 0.10	0.5%	8.82 ± 0.06	99.5%	0.71×10^4	1.06×10^5
[CuL(PPh$_3$)I]	559	0.294	1.22 ± 0.18	1%	11.6 ± 0.16	99%	2.53×10^4	0.61×10^5

nonradiative decay in the solid state can be understood as follows. The possibilities for the excited state conformation change from tetrahedral geometry to a flattening one as well as molecular vibrations and rotations, are restricted in the rigid medium in comparison with the solution.[6]

For the solid samples, the PLQY and lifetimes increase in the order **1** < **2** < **3** (Table 4) so that the luminescence for **3** is greatly enhanced in comparison with its bromido- and chlorido-analogs. This results from the noticeable increase of radiative decay and simultaneous suppression of nonradiative decay. It was shown that nonradiative decay depends on the degree of the excited state distortion.[23] The small Stokes shifts are indicative of the effective suppression of geometric relaxation in the ^{3}MLCT excited state. This means that the degree of excited state distortion decreases on going from the chlorido- to iodido-complex. Importantly, this tendency correlates with the tendency of pseudo-tetrahedral coordination sphere of the complexes to become more symmetric in the same order. As far as electronic factors are concerned, the sequence of π-accepting properties of halide ions (Cl^- < Br^- < I^-) may contribute to the increase in the energy gap between the excited and ground states thus increasing excited state lifetimes and PLQY.

Adachi with colleagues have recently stated that nonradiative decay can be suppressed not only by reducing excited-state distortion but also by reducing C–H vibrational quenching.[24] We have shown that the lowering of vibrational frequencies of the CH- and CH_2-groups and heteroaromatic rings takes place on going from the chlorido- to iodido-complex. In addition, frequencies of Cu–N and Cu–Hal vibrations decrease in the same order. These data provide additional evidence to support the strategy of suppressing vibrational quenching.

Conclusion

We synthesized a series of heteroleptic mononuclear copper(I) complexes, [CuL(PPh_3)Cl], [CuL(PPh_3)Br], and [CuL(PPh_3)I], and demonstrated that coordinated halide ions strongly affect their luminescent behavior. In CH_2Cl_2 solutions, the complexes display intensive LL* luminescence with short lifetimes of about 2 ns. The ^{3}MLCT luminescence is either weak (for [CuL(PPh_3)I]) or absent (for [CuL(PPh_3)Cl]). However, in the solid state, the complexes demonstrate bright ^{3}MLCT luminescence in a yellow–red spectral range with a long lifetime in microsecond intervals. The PL quantum yield and excited state lifetimes increase in the order [CuL(PPh_3)Cl] < [CuL(PPh_3)Br] < [CuL(PPh_3)I]. The degree of distortion of the pseudo-tetrahedral CuN_2PHal core determined from X-ray single crystal data and the Stokes shift being an indicator of the degree of excited state distortion decrease in the same order. Furthermore, the bands in IR spectra shift to low frequencies on going from the chlorido- to iodido-complex. Thereby, the suppression of vibrational quenching also contributes to the improvement of PL quantum efficiency.

Acknowledgements

The authors are grateful to Anna P. Zubareva, Olga S. Koscheeva, and Evgenii M. Uskov for their help and useful discussions. The work was financially supported by Russian Foundation for Basic Research (Project 12-03-31266 mol_a).

Notes and references

1 D. R. McMillin and K. M. McNett, *Chem. Rev.*, 1998, **98**, 1201; V. W.-W. Yam and K. K.-W. Lo, *Chem. Soc. Rev.*, 1999, **28**, 323; N. Armaroli, G. Accorsi, F. Cardinali and A. Listorti, *Top. Curr. Chem.*, 2007, **280**, 69; A. Barbieri, G. Accorsi and N. Armaroli, *Chem. Commun.*, 2008, 2185; R. Peng, M. Li and D. Li, *Coord. Chem. Rev.*, 2010, **254**, 1; M. Vitale and P. C. Ford, *Coord. Chem. Rev.*, 2011, **219–221**, 3; V. W.-W. Yam and K. M.-C. Wong, *Chem. Commun.*, 2011, **47**, 11579; K. Tsuge, *Chem. Lett.*, 2013, **42**, 204.

2 R. Czerwieniec, J. Yu and H. Yersin, *Inorg. Chem.*, 2011, **50**, 8293; J. Min, Q. Zhang, W. Sun, Y. Cheng and L. Wang, *Dalton Trans.*, 2011, **40**, 686.

3 L. Shi, B. Li, S. Lu, D. Zhu and W. Li, *Appl. Organomet. Chem.*, 2009, **23**, 379; J. Sun, *J. Lumin.*, 2012, **132**, 1515.

4 J.-L. Chen, P. Song, J. Liao, H.-R. Wen, R. Hong, Z.-N. Chen and Y. Chi, *Inorg. Chem. Commun.*, 2010, **13**, 1057; W. Wei, M. Wu, Q. Gao, Q. Zhang, Y. Huang, F. Jiang and M. Hong, *Inorg. Chem.*, 2009, **48**, 420.

5 L. Bergmann, J. Friedrichs, M. Mydlak, T. Baumann, M. Nieger and S. Bräse, *Chem. Commun.*, 2013, **49**, 6501; R. Czerwieniec, K. Kowalski and H. Yersin, *Dalton Trans.*, 2013, **42**, 9826; C. Femoni, S. Muzzioli, A. Palazzi, S. Stagni, S. Zacchini, F. Monti, G. Accorsi, M. Bolognesi, N. Armaroli, M. Massi, G. Valenti and M. Marcaccio, *Dalton Trans.*, 2013, **42**, 997; J.-J. Cid, J. Mohanraj, M. Mohankumar, M. Holler, G. Accorsi, L. Brelot, I. Nierengarten, O. Moudam, A. Kaeser, B. Delavaux-Nicot, N. Armaroli and J.-F. Nierengarten, *Chem. Commun.*, 2013, **49**, 859; L.-F. Shi, B. Li, L.-M. Zhang, Q.-H. Zuo and S. Yue, *Inorg. Chim. Acta*, 2013, **400**, 91; I. Andrés-Tomé, J. Fyson, F. B. Dias, A. P. Monkman, G. Iacobellis and P. Coppo, *Dalton Trans.*, 2012, **41**, 8669; F. Wei, L. Wang and Y. Huang, *Inorg. Chim. Acta*, 2010, **363**, 2600; S. B. Harkins and J. C. Peters, *J. Am. Chem. Soc.*, 2005, **127**, 2030.

6 L. Qin, Q. Zhang, W. Sun, J. Wang, C. Lu, Y. Cheng and L. Wang, *Dalton Trans.*, 2009, 9388.

7 T. Hou, J. Bian, X. Yue, S. Yue and J. Ma, *Inorg. Chim. Acta*, 2013, **394**, 15; X. Liu, H. Nan, W. Sun, Q. Zhang, M. Zhan, L. Zou, Z. Xie, X. Li, C. Lu and Y. Cheng, *Dalton Trans.*, 2012, **41**, 10199; X.-L. Li, Y.-B. Ai, B. Yang, J. Chen, M. Tan, X.-L. Xin and Y.-H. Shi, *Polyhedron*, 2012, **35**, 47; E. S. Smirnova, A. A. Melekhova, V. V. Gurzhiy, S. I. Selivanov, D. V. Krupenya, I. O. Koshevoy and S. P. Tunik, *Z. Anorg. Allg. Chem.*, 2012, **638**, 415; K. Saito, T. Arai, N. Takahashi, T. Tsukuda and T. Tsubomura, *Dalton Trans.*, 2006, 4444; D. G. Cuttel, S.-M. Kuang,

P. E. Fanwick, D. R. McMillin and R. A. Walton, *J. Am. Chem. Soc.*, 2002, **124**, 6; R. A. Rader, D. R. McMillin, M. T. Buckner, T. G. Matthews, D. J. Casadonte, R. K. Lengel, S. B. Whittaker, L. M. Darmon and F. E. Lytle, *J. Am. Chem. Soc.*, 1981, **103**, 5906.

8 C. Hirtenlehner and U. Monkowius, *Inorg. Chem. Commun.*, 2012, **15**, 109; H. Araki, K. Tsuge, Y. Sasaki, S. Ishizaka and N. Kitamura, *Inorg. Chem.*, 2005, **44**, 9667.

9 S. Achelle and N. Plé, *Curr. Org. Synth.*, 2012, **9**, 163.

10 M. Kidwai, S. Saxena, S. Rastogi and R. Venkaramanan, *Curr. Med. Chem. – Anti-Infect. Agents*, 2003, **2**, 269.

11 K. A. Vinogradova, V. P. Krivopalov, E. B. Nikolaenkova, N. V. Pervukhina, D. Yu. Naumov, M. I. Rakhmanova, E. G. Boguslavsky, L. A. Sheludyakova and M. B. Bushuev, *Polyhedron*, 2013, **57**, 1.

12 N. Saha and D. Mukherjee, *Inorg. Chim. Acta – Bioinorg. Chem.*, 1987, **137**, 161; L. Soto, J. Garcia, E. Escriva, J.-P. Legros, J.-P. Tuchagues, F. Dahan and A. Fuertes, *Inorg. Chem.*, 1989, **28**, 3378.

13 P. J. Steel and E. C. Constable, *J. Chem. Res., Synop.*, 1989, 189; P. J. Steel and E. C. Constable, *J. Chem. Soc., Dalton Trans.*, 1990, 1389.

14 A. Jana, S. Konar, K. Das, S. Ray, J. A. Golen, A. L. Rheingold, J. Ribas, M. S. El Fallah and S. K. Kar, *Polyhedron*, 2012, **47**, 24; T. Ishida, K. Yanagi and T. Nogami, *Inorg. Chem.*, 2005, **44**, 7307.

15 M. C. Carrión, I. M. Ortiz, F. A. Jalón, B. R. Manzano, A. M. Rodríguez and J. Elguero, *Cryst. Growth Des.*, 2011, **11**, 1766; A. Jana, S. Konar, K. Das, S. Ray, J. A. Golen, A. L. Rheingold, L. M. Carrella, E. Rentschler, T. K. Mondal and S. K. Kar, *Polyhedron*, 2012, **38**, 258; P. Cañellas, M. Torres, A. Bauzá, M. M. Cánaves, K. Sánchez, M. I. Cabra, A. García-Raso, J. J. Fiol, P. M. Deyà, E. Molins, I. Mata and A. Frontera, *Eur. J. Inorg. Chem.*, 2012, **2012**, 3995; P. Cañellas, A. Bauzá, A. García-Raso, J. J. Fiol, P. M. Deyà, E. Molins, I. Mata and A. Frontera, *Dalton Trans.*, 2012, **41**, 11161; K. T. Prasad, B. Therrien, S. Geib and K. M. Rao, *J. Organomet. Chem.*, 2010, **695**, 495.

16 M. B. Bushuev, V. P. Krivopalov, N. V. Pervukhina, D. Yu. Naumov, G. G. Moskalenko, K. A. Vinogradova, L. A. Sheludyakova and S. V. Larionov, *Inorg. Chim. Acta*, 2010, **363**, 1547.

17 E. Brunet, O. Juanes, R. Sedano and J. C. Rodríguez-Ubis, *Tetrahedron Lett.*, 2007, **48**, 1091.

18 L.-H. He, J.-L. Chen, F. Zhang, X.-F. Cao, X.-Z. Tan, X.-X. Chen, G. Rong, P. Luo and H.-R. Wen, *Inorg. Chem. Commun.*, 2012, **21**, 125; J.-L. Chen, X.-F. Cao, W. Gu, B.-T. Su, F. Zhang, H.-R. Wen and R. Hong, *Inorg. Chem. Commun.*, 2012, **15**, 65; L. H. He, J. L. Chen, J. Y. Wang, X. X. Chen, X. Z. Tan and X. F. Cao, *Chin. Chem. Lett.*, 2012, **23**, 1169; Y.-L. Xiao, Q.-H. Jin, Y.-H. Deng, Z.-F. Li, W. Yang, M.-H. Wu and C.-L. Zhang, *Inorg. Chem. Commun.*, 2012, **15**, 146; R. Starosta, U. K. Komarnicka, M. Puchalska and M. Barys, *New J. Chem.*, 2012, **36**, 1673; R. Starosta, M. Puchalska, J. Cybińska, M. Barys and A. V. Mudring, *Dalton Trans.*, 2011, **40**, 2459; J.-L. Chen, P. Song, J. Liao, H.-R. Wen, R. Hong, Z.-N. Chen and Y. Chi, *Inorg. Chem. Commun.*, 2010, **13**, 1057.

19 G. T. Wright, *Proc. Phys. Soc. B*, 1955, 241.

20 *APEX2 (Version 1.08), SAINT (Version 7.03), and SADABS (Version 2.11). Bruker Advanced X-ray Solutions*, Bruker AXS Inc., Madison, Wisconsin, USA, 2004; G. M. Sheldrick, *SHELX97 Release 97-2*, University of Göttingen, Germany, 1998.

21 C. C. Phifer and D. R. McMillin, *Inorg. Chem.*, 1986, **25**, 1329.

22 A. Makal, J. Benedict, E. Trzop, J. Sokolow, B. Fournier, Y. Chen, J. A. Kalinowski, T. Graber, R. Henning and P. Coppens, *J. Phys. Chem.*, 2012, **116**, 3359; P. Coppens, J. Sokolow, E. Trzop, A. Makal and Y. Chen, *J. Phys. Chem. Lett.*, 2013, **4**, 579.

23 E. C. Riesgo, Y.-Z. Hu, F. Bouvier, R. P. Thummel, D. V. Scaltrito and G. J. Meyer, *Inorg. Chem.*, 2001, **40**, 3413.

24 A. Wada, Q. Zhang, T. Yasuda, I. Takasu, S. Enomoto and C. Adachi, *Chem. Commun.*, 2012, **48**, 5340.

